

METAL RECOVERY AND REMEDIATION OF MINE WATER EFFLUENT FROM SIDERITE DEPOSIT NIŽNÁ SLANÁ, EASTERN SLOVAKIA

Daniel Kupka¹, Zuzana Bártová^{1*}, Lenka Hagarová¹, Inna Melnyk¹, Viktoriia Kyshkarova¹ Eva Mačingová¹, Josef Zeman²

¹*Institute of Geotechnics of the Slovak Academy of Sciences, Watsonova 45, 040 01 Kosice, Slovakia*

²*Masaryk University, Kotlářská 2, 611 37 Brno, Czech Republic*

ABSTRACT

Mine impacted water discharged from the flooded deposit of siderite ores in Nižná Slaná (situated in the region of the Ore Mts., Eastern Slovakia) transport a huge amount of metals, metalloids and sulfate anions to the river recipient, representing the environmental risk for the river itself and surrounding regions. On the other hand, it offers appreciable source of metals, potentially usable in further applications.

The idea of using anoxic limestone drains (ALD) as alkalinity generators prior to passive treatment systems was considered. Unfortunately, mine water from the deposit is highly supersaturated with respect to ferric iron (oxy)hydroxides and alkali metal jarosites. Appreciable concentrations of dissolved Fe^{2+} or Al^{3+} would result in precipitation and coating of limestone surfaces and in rapid clogging of the interstitial spaces. In addition, high sulfate concentration of the water ($> 30g/L$) would cause problems with clogging of ALD drains due to gypsum precipitation.

This work presents (discusses) two active approaches to AMD treatment; one with oxidation of Fe^{2+} to Fe^{3+} using Fe-oxidizing bacteria followed by precipitation of iron in the trivalent form, and the other process without oxidation step, using lime to neutralize the acidity and precipitate Fe^{2+} in the form of $Fe(OH)_2$. The iron-precipitation/sedimentation step, is followed by oxidative precipitation of Mn and a purification and recovery system using a selective chelating resin and composite adsorbents to recover high value constituents (Ni, Co,) in a high-quality form and purify water from other toxic elements (As, Cd). The recovery of metals from mine-impacted water (MIW) not only reduces environmental impacts but also provides a source of valuable resources.

Keywords: Fe-oxidizing bacteria, iron oxidation, passive/ active approaches, metals recovery, acid mine drainage, mine impacted waters

Abbreviations:

ALD	anoxic limestone drains
AMD	acid mine drainage
FBR	fluid bed reactor
HRT	hydraulic retention time
MIW	mine-impacted water

1 Introduction

The mine water effluent from the former mining plant Siderit Nižná Slaná (Fig. 1) is an active source of pollution of the Slaná River. The high iron content causes a significant red coloration of the river, which is observed several tens of km in the direction of the water flow (Fig. 2). Ferric iron precipitates are further transported downstream for a long distance and accumulate in places where the kinetic energy of the water flow is reduced. Mine water from the deposit is highly supersaturated with respect to ferric hydroxide and alkali metal jarosites.

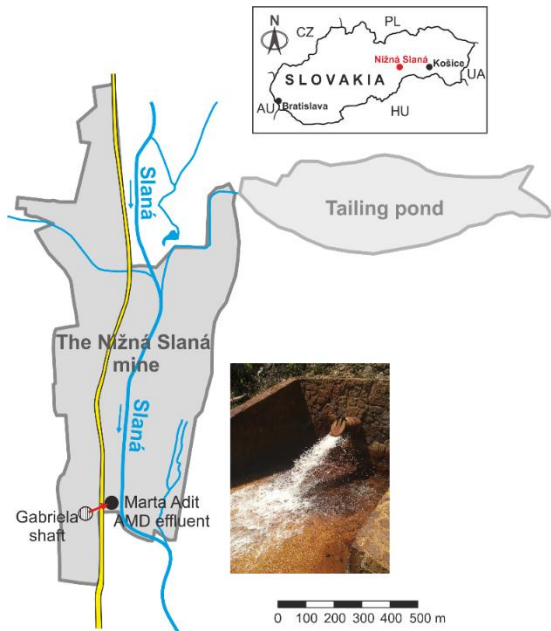


Fig. 1. Location of the former mining plant Siderit Nižná Slaná and its discharge into Slaná river

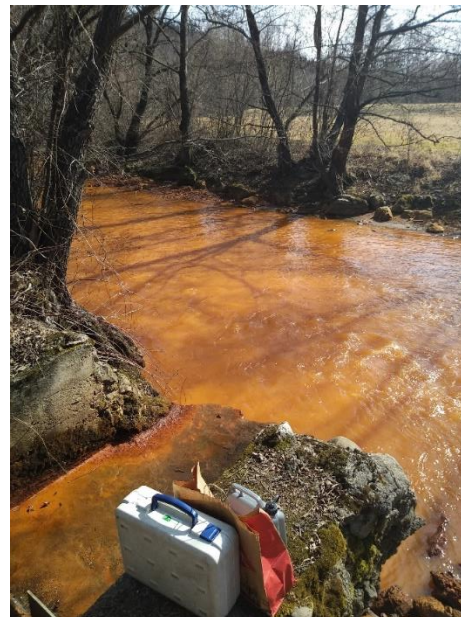


Fig. 2. Intensive red coloration of the Slaná river observable several tens of km in the direction of the water flow

Treatment of Mine-Impacted Water (MIW) is essential to minimize its impact on the environment and protect public health. The choice of treatment method depends on the geochemical characteristics of the mine water and the environmental regulations in place (Kirby and Cravotta, 2005; Mogashane et al., 2020). AMD treatment technologies are categorized as passive and active (García et al., 2001). Both treatment approaches are effective in reducing toxic metals and sulfate concentrations and in lowering acidity via generating alkalinity (Johnson and Hallberg, 2005).

In this work, two active approaches to AMD treatment are being considered; one with oxidation of Fe^{2+} to Fe^{3+} using Fe-oxidizing bacteria followed by precipitation of Fe in the trivalent form, and

the other process without Fe^{2+} oxidation using lime to neutralize the acidity and precipitate Fe^{2+} in the form of $\text{Fe}(\text{OH})_2$. The first technology proposed here consists of intensive oxidation of divalent iron to trivalent form and controlled precipitation of $\text{Fe}(\text{III})$ at low pH in the form of suitable minerals with their subsequent separation using sedimentation or filtration (Fig. 3 A). The pre-treated (still acidic) solution is then passed through a bed of ion-exchange resin. The resin selectively binds to the metal ions in the solution. The type of adsorption material depends on the specific characteristics of the MIW and the metals present. Chelating resins are a type of ion exchangers that can selectively remove metals from polymetallic solutions. These resins contain ligands that have a high affinity for metal ions, which can be selectively removed from the solution. The resin becomes saturated with metal ions over time and needs to be regenerated to be reused. This is typically done by washing the resin with a regenerant solution, which displaces the metal ions from the resin. A necessary requirement is also to reduce the concentration of sulfates and eliminate the acidity of mine water with neutralizing substances.

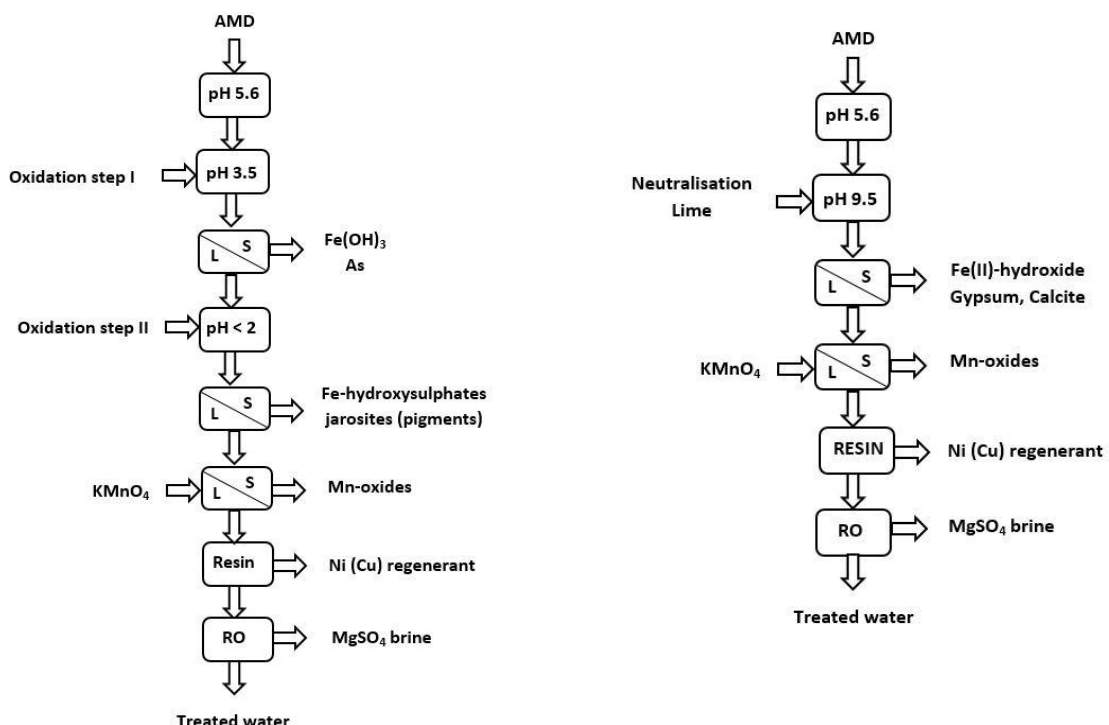


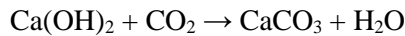
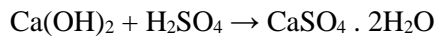
Fig. 3. Two active approaches to AMD treatment. **Left-** approach with oxidation of Fe^{2+} to Fe^{3+} using Fe -oxidizing bacteria followed by precipitation of Fe in the trivalent form; **Right-** process without Fe^{2+} oxidation using lime to neutralize the acidity and precipitate Fe^{2+} in the form of $\text{Fe}(\text{OH})_2$

1.1 AMD neutralization by lime

Neutralization of acid mine drainage (AMD) by limestone proved to be effective in various laboratory tests and real-scale applications worldwide (Brahaita et al., 2017). Although many different biological and chemical technologies exist for treatment of AMD, lime neutralization remains by far the most widely applied method. This is largely due to the high efficiency in removing dissolved metals through neutralization, combined with the fact that lime costs are low in comparison to alternatives. Lime treatment essentially consists in bringing the pH of the AMD to a point where the metals of concern are insoluble and precipitate (Fig 3. B). A subsequent separation of these precipitates is then required to produce a clear effluent which meets regional discharge criteria.

The principle of lime neutralization lies in the insolubility of heavy metals in alkaline conditions. By controlling the pH to a typical set point of about 9.5, metals such as iron (Fe), zinc (Zn), and copper (Cu) are precipitated. Other metals such as nickel (Ni) and cadmium (Cd) require a higher pH, in the range of 10.5 to 11 to effectively precipitate the hydroxides. A common by-product

of lime neutralization is gypsum. Another common by-product of lime neutralization is calcium carbonate.



In this procedure, the major constituent iron and partly sulfates are precipitated and separated in the first step, and in subsequent steps Mn and Ni are recovered from the alkaline solution.

2 Materials and methods

2.1 Sampling and Chemical analyses

Samples of mine water were collected from the Gabriela shaft that receives the majority of waters draining the flooded mine area. Samples for iron speciation were filtered immediately through 0.2 µm (pore size) membrane filters and acidified with H₂SO₄. The second collection for chemical analysis was unfiltered and stabilized with HNO₃.

Concentration of metals in mine water was determined using atomic absorption spectrometer VARIAN AA240FS. Sulfate concentration was analysed by ion chromatography Dionex ICS 5000. Ferric iron was determined by a UV-spectrophotometric method at 300 nm (Basaran and Tuovinen, 1986). Ferrous iron concentrations were determined by modified o-phenanthroline spectrophotometric method, insensitive to Fe(III) interference (Herrera et al., 1989).

2.2 Acidity and alkalinity determination

Acidity was determined by “hot peroxide” titration method by boiling a 50 mL sample with 1 mL of 30% H₂O₂ and titrating it to pH 8.3 with 0.1 N NaOH. Alkalinity was measured by titrating a 50 mL sample with 0.2 N H₂SO₄ to pH 4.8. A combined glass electrode with a built-in reference electrode (Ag/AgCl) was used for pH measurement. The ORP of the solutions was measured with a platinum redox electrode with a built-in reference electrode (Ag/AgCl). In both cases, a device (PHM 210 METERLAB, France) was used.

2.3 Bacterial strains and incubation conditions

Two strains of chemolithotrophic, iron-oxidizing bacteria were used in the experiments: *Acidithiobacillus ferrovorans* SS3 (DSM 17398) and *Leptospirillum feriphilum* (DSM 14647). The cultures were maintained in a liquid mineral medium that contained: 1.6 mM MgSO₄ · 7H₂O, 6.1 mM (NH₄)₂PO₄, 0.23 mM K₂HPO₄ and 120 mM FeSO₄ · 7H₂O in 4 mM H₂SO₄ at 25 °C in aerobic conditions in a batch mode.

2.4 Gas analysis

The on-line measurement of the oxygen and carbon dioxide consumption/production from the gas-phase was used to measure the chemical (abiotic) and bacterial ferrous iron oxidation rate and the rate of bacterial growth. Paramagnetic oxygen analyser (PA-10a) and infrared carbon dioxide analyser (CA-10 Sable Systems) were used for O₂ and CO₂ analyses in inlet and outlet air respectively. The analyzers were calibrated for zero (99.99 % N₂) and ambient air O₂ and CO₂ concentrations span. The data acquisition was performed by a software application developed in LabVIEW ® (National Instruments).

2.5 Geochemical modelling

Geochemical modelling of mine water and the processes that take place during AMD equilibration with the atmosphere and AMD alkalization was carried out in the suite of programs Geochemist's Workbench® 2022.

3 Results

3.1 Physico-chemical parameters of mine water

The mine water is of magnesium-sulfate type with a high concentration of dissolved iron and high total mineralization (concentration of dissolved substances $\sim 53 \text{ g L}^{-1}$). Major elements are: magnesium $\text{Mg}^{2+} \sim 5.5 \text{ g L}^{-1}$, dissolved ferrous iron $\text{Fe}^{2+} \sim 5 \text{ g L}^{-1}$, manganese $\text{Mn}^{2+} \sim 0.6 \text{ g L}^{-1}$. Of the anions, the most abundant are sulfates $\sim 35 \text{ g L}^{-1}$ and bicarbonates (Tab. 1). At a flow rate of $\sim 20 \text{ l s}^{-1}$ ($72 \text{ m}^3 \text{ h}^{-1}$), the approximate balance of pollutants flowing to the Slaná recipient is $\sim 90 \text{ t}$ per day. Mine water has an acidic reaction, pH 5.7, and has acidity in excess of alkalinity (net acidity $\sim 160 - 180 \text{ mmol L}^{-1}$). When mixed with water from the Slaná River, approximately 52 liters of river water is needed to neutralize 1 liter of mine water. Water after discharge from the mining environment is subject to rapid chemical changes. The pH, alkalinity, and associated properties change as the water equilibrates to atmospheric conditions because of the degassing of dissolved carbon dioxide, oxidation of Fe^{2+} and Mn^{2+} , and hydrolysis of Fe^{3+} and Mn^{4+} . The instability of the sample results from the fact that the chemical reactions that create equilibrium between the gas, water, and solid phases in the system occur at different rates. The pH ultimately decreases to acidic values and the turbidity and red colouring of the water increase because of the oxidation of Fe^{2+} and the consequent precipitation of Fe(OH)_3 .

Table 1. The physical-chemical parameters of mine water from Nižná Slaná

pH	ORP (mV)	Mn (mg/l)	Fe^{2+} (mg/l)	Mn (mg/l)	Mg (mg/l)	SO_4^{2-} (mg/l)	As (mg/l)	Ni (mg/l)	Co (mg/l)
5.60	-6.70	533	4 762	533	5 492	35 796	14.67	15.90	3.6

3.2 Oxidation of Fe in natural fresh waters

The rate of Fe^{2+} chemical oxidation by molecular oxygen is dependent on the pH value of the mine water. Hydrolysed species of divalent iron Fe(OH)^+ and Fe(OH)_2^0 undergo oxidation much faster than Fe^{2+} ion.

$$\frac{-d[\text{Fe}^{2+}]}{dt} = (k_0[\text{Fe}^{2+}] + k_1[\text{Fe(OH)}^+] + k_2[\text{Fe(OH)}_2^0]) pO_2$$

The values of the rate constants differ from each other by 5 orders of magnitude $k_0 = 6 \times 10^{-5}$; $k_1 = 1.7$; $k_2 = 4.3 \times 10^5 \text{ min}^{-1}$. The overall rate of iron oxidation depends dramatically on the pH-dependent distribution of these three species in the aqueous phase (Singer and Stumm, 1970).

In waters with a pH value > 5 , the rate of iron oxidation is directly proportional to the concentration of Fe^{2+} and the partial pressure of oxygen, and increases proportionally to the square of the $[\text{OH}^-]$ ion concentration.

$$\frac{-d[\text{Fe}^{2+}]}{dt} = k[\text{Fe}^{2+}][\text{OH}^-]^2 pO_2$$

The rate of Fe^{2+} oxidation in pH-neutral waters is high with half-times of the order of minutes. At pH values < 4 , the rate decreases dramatically. In solutions with pH < 3 , the rate of iron oxidation is extremely slow.

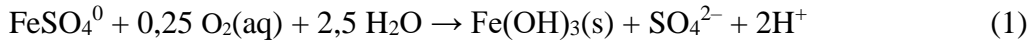
In acidic sulfate solutions, the rate is directly proportional to the partial pressure of oxygen and proportional to the square of the Fe^{2+} concentration.

$$\frac{-d[\text{Fe}^{2+}]}{dt} = k_3[\text{Fe}^{2+}]^2 pO_2$$

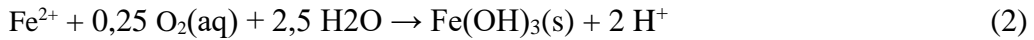
3.3 Geochemical modelling of Fe oxidation in mine water

Geochemical modelling was used to assess the processes that take place during AMD equilibration with the atmosphere and AMD alkalization and to assess the stability fields of the precipitated minerals. The reaction of oxidation of divalent iron by molecular oxygen is described by chemical equations 1-4.

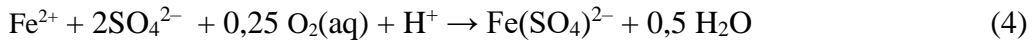
Oxidation of sulfate complex FeSO_4^0 :



Oxidation of free ions Fe^{2+} :



A significant part of trivalent iron remains in mine water in the form of sulfate complexes:



The H^+ ion, which is a product of hydrolytic reactions, causes a decrease in the $\text{pH} < 3$. After consuming approximately 22 mmol of dissolved oxygen $\text{O}_2(\text{aq})$, practically all the divalent iron in the mine water is oxidized to trivalent iron. The resulting balance between FeSO_4^+ and ferric hydroxide Fe(OH)_3 is described by a chemical equation:



The results of geochemical modelling of iron oxidation and precipitation of Fe(OH)_3 in model mine water are shown in Fig. 4.

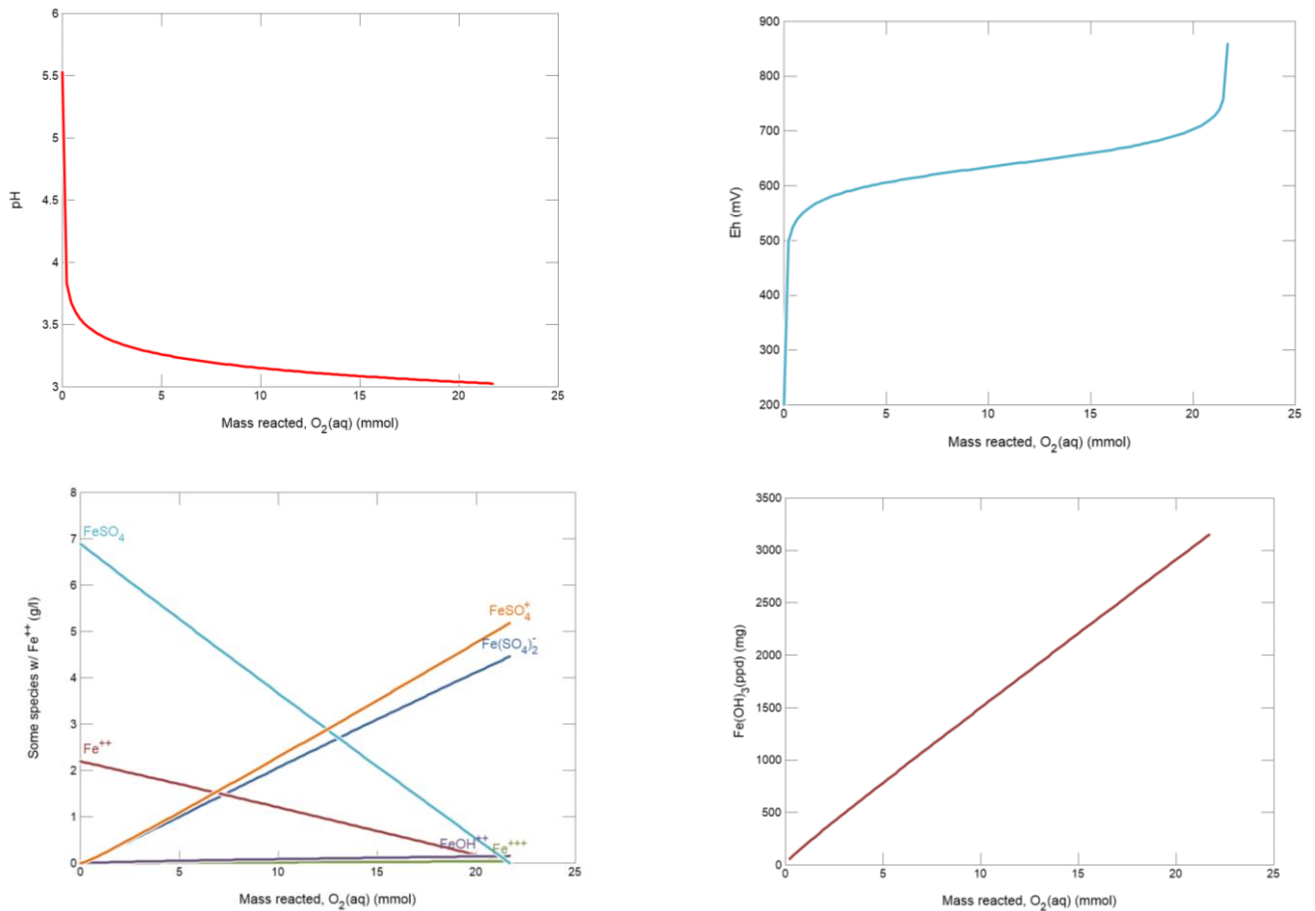


Fig. 4. Geochemical model: Change in pH, Eh, concentration of dissolved iron species and precipitation of amorphous iron hydroxide during model mine water oxidation

After oxidation by atmospheric oxygen, the pH value drops to 2.37 due to the oxidation of divalent iron to trivalent iron and the formation of the $\text{Fe}(\text{OH})^{2+}$ complex, which is the most abundant species of trivalent iron in water in the given pH range.



This was verified by accelerated oxidation of mine water with hydrogen peroxide, when the pH value dropped to values around 2.0–2.2. Although divalent iron is oxidized to trivalent iron, precipitation of goethite practically does not occur, because the solubility of goethite increases with decreasing pH, and the change in pH-Eh conditions follows the equilibrium line between the sulfate complex FeSO_4 and goethite.

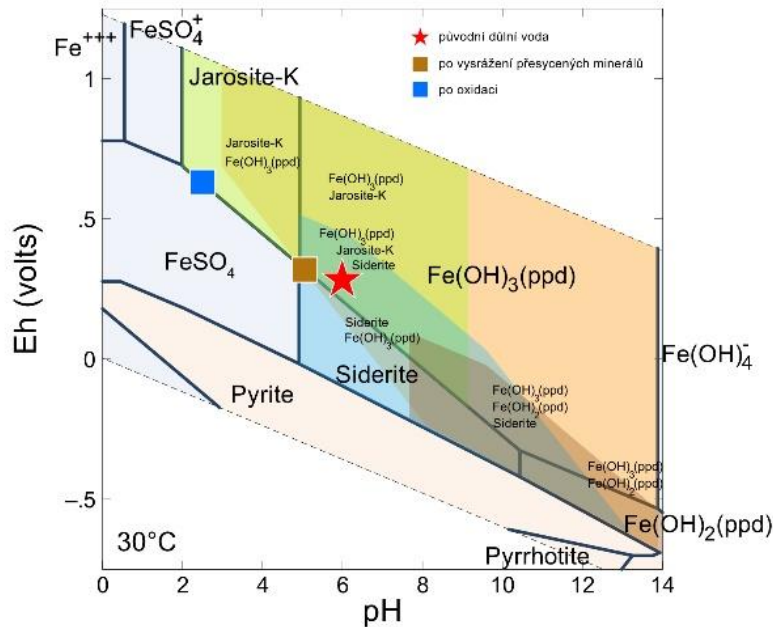


Fig. 5. Speciation diagram for mine water from Nižná Slaná. The diagram was constructed for the activities of the constituents in the actual sample of mine water. The red asterisk symbol indicates initial conditions of mine water from the Gabriela shaft. The blue square indicates conditions after Fe oxidation. The coloured fields indicate areas of conditions under which the mine water is supersaturated with respect to individual minerals

The interconversions of iron minerals modify the mobility and environmental impact of adsorbed and co-precipitated elements. While such conditions may be predicted from geochemical speciation models using appropriate thermodynamic parameters, the paragenetic pathways of mineral formation are often driven by kinetics.

3.4 Oxidation of Fe in mine water from Nižná Slaná in equilibrium with atmospheric air

Before the use of selective ion exchanger, the major element Fe should be removed first. The MIW is further treated to remove any suspended solids or other impurities that may interfere with the recovery process with ion exchanger. Mn oxidation occurs more slowly than Fe oxidation, and is sensitive to the presence of Fe^{2+} , which will inhibit or reverse Mn^{2+} oxidation.

Iron oxidation in the actual sample of mine water during the aeration was monitored using online gas analysis and liquid phase chemical analysis. The rate of iron oxidation was calculated from the oxygen consumption rate, using the stoichiometry of equation 1. The initial rapid abiotic oxidation of ferrous iron in aerated water becomes increasingly slower as pH decreases, especially below ca. pH 3.5. Fig. 5. shows the evolution of the oxidation rate of iron in mine water under laboratory conditions at a temperature of 30 °C. The rate of Fe^{2+} oxidation decreased from an initial value of $>1000 \text{ mg L}^{-1} \text{ h}^{-1}$ (pH 5.5) to a value of $\sim 5 \text{ mg L}^{-1} \text{ h}^{-1}$ at pH < 3 . The total amount of oxidized iron in 25 h is approximately 450 mg L^{-1} , which is less than 10% of the initial Fe^{2+} concentration.

When the pH value drops < 3 , a significant part of the ferric iron remains dissolved in the mine water in the form of sulfate complexes, and with the continued oxidation of Fe^{2+} , the concentration of the dissolved Fe^{3+} ion in the solution gradually increases. After the complete oxidation of Fe^{2+} to Fe^{3+} , the pH of the mine water drops to a value of pH < 2 (Fig. 6.).

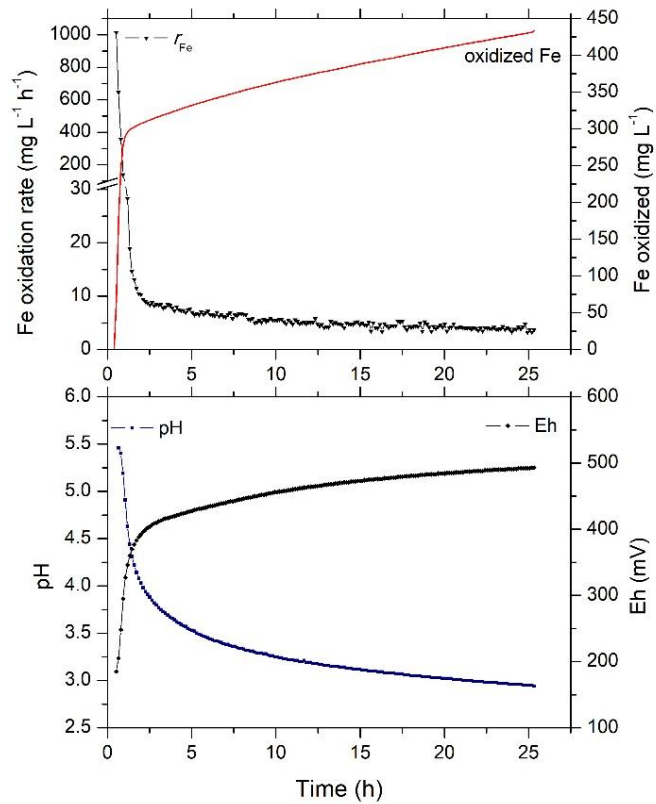


Fig.6. Abiotic oxidation of ferrous iron in mine water from Nižná Slaná by atmospheric oxygen. Change in pH and oxidation-reduction potential (Eh). The rate of iron oxidation decreases sharply at $pH < 4$

Oxidation of divalent iron, which is present in the form of the sulfate complex FeSO_4^0 and free Fe^{2+} ions, and the subsequent hydrolysis and precipitation of Fe^{3+} species causes significant acidification of the mine water. The oxidation-reduction potential of samples of mine water taken from the Gabriela pit (anoxic conditions) relative to the hydrogen reference electrode (Eh) has values < 200 mV. By changing the $\text{Fe}^{3+}/\text{Fe}^{2+}$ ratio during iron oxidation, the oxidation-reduction potential increases to ~ 900 mV (Fig. 7.).

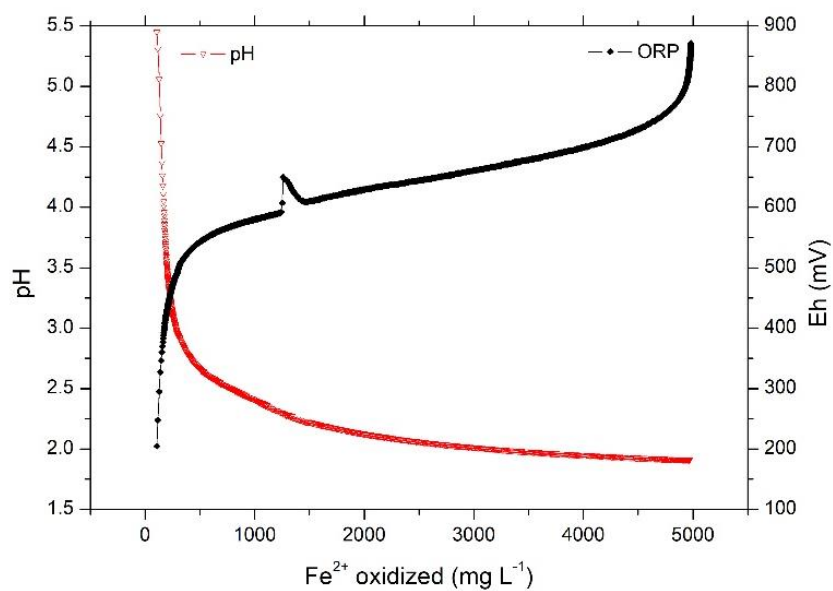


Fig. 7. Change in pH and oxidation-reduction potential of mine water during the oxidation of Fe^{2+} to Fe^{3+}

Changes in pH and Eh during Fe oxidation in actual sample of mine water are analogous to the results obtained by geochemical modelling. The quantity and quality of the resulting precipitation product depends on the rate of precipitation of individual minerals. During the fast oxidation of iron with hydrogen peroxide, the final concentration of soluble ferric species stabilizes at a value of approximately 2-2.5 g L^{-1} . Approximately equal amounts of ferric iron precipitated in the form of iron hydroxide (Fig. 8.).

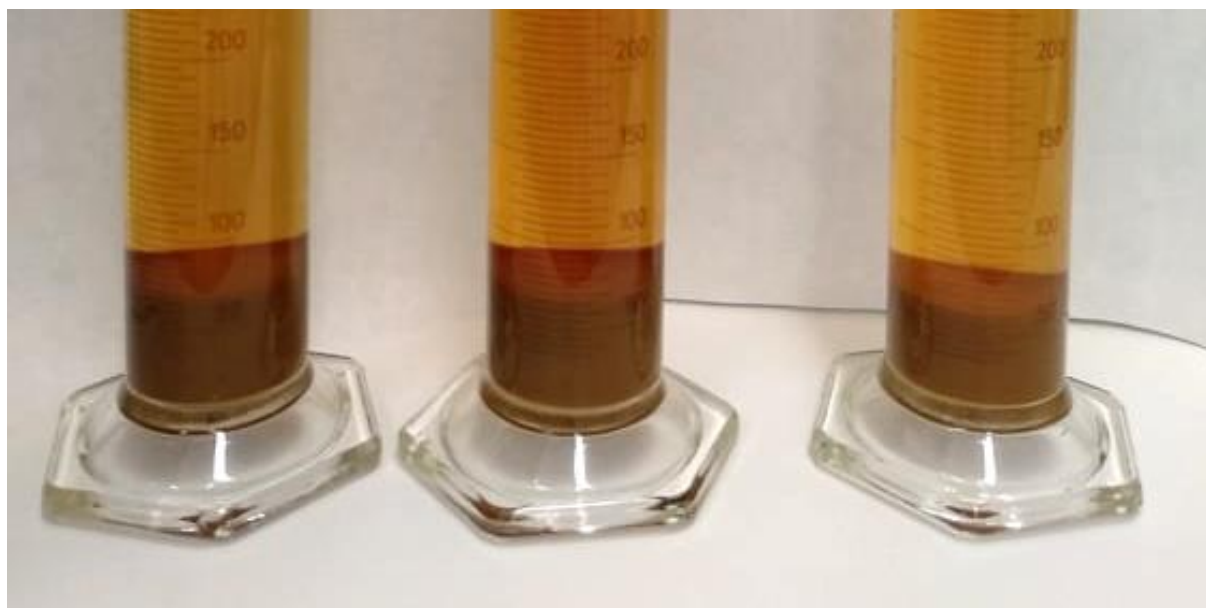


Fig. 8. Mine water after rapid oxidation of Fe^{2+} to Fe^{3+} by H_2O_2 . Initial concentration of $\text{Fe}^{2+} \sim 5000 \text{ mg L}^{-1}$. The concentration of dissolved Fe^{3+} in the solution $\sim 2500 \text{ mg L}^{-1}$

By adjusting the pH > 6, the rate of iron oxidation increases by several orders of magnitude. Such an increase in the oxidation rate of Fe^{2+} can be observed after mixing the waters in the Slaná recipient after neutralizing the acidic mine water with river water containing alkalinity and dissolved oxygen.

3.5 Bacterial oxidation of iron in mine water

Iron-oxidizing bacteria have efficient enzymatic systems that catalyse the oxidation of Fe^{2+} , enable the transfer of electrons from Fe^{2+} to O_2 and the use of energy from this oxidation reaction for growth and metabolic processes in the cell. The rate of Fe^{2+} oxidation in an acidic environment increases in direct proportion to the number of bacterial cells (enzymes) per unit volume. They are mostly autotrophic organisms that are capable of metabolizing atmospheric CO_2 into organic compounds. Therefore, it is not necessary to provide them with another source of carbon, which is important especially from the application point of view. Air is also the source of the terminal acceptor of electrons - oxygen.

Fig. 9 shows the behaviour of the oxygen consumption rate (oxidation of Fe^{2+}), CO_2 degassing and changes in oxidation-reduction potential and pH of mine water during equilibration with atmosphere. During the first 25 hours, chemical oxidation of iron took place with a typical decrease in pH and subsequent decrease in the rate of Fe oxidation. The reaction liquor was then inoculated with a pure culture of *L. ferriphilum* and the reactor was run in batch mode until complete oxidation of Fe^{2+} to Fe^{3+} at $t = 30^\circ\text{C}$. After the inoculation of iron-oxidizing bacteria (at time $t = 25$ h), there is a sudden increase in the rate of Fe oxidation, followed by exponential increase proportional to the exponential growth of bacterial culture. The conditions of the experiment made it possible to measure the net consumption of CO_2 by the bacteria, because of equilibration with the atmosphere and the low pH value, when only the solubility of gaseous CO_2 comes into consideration.

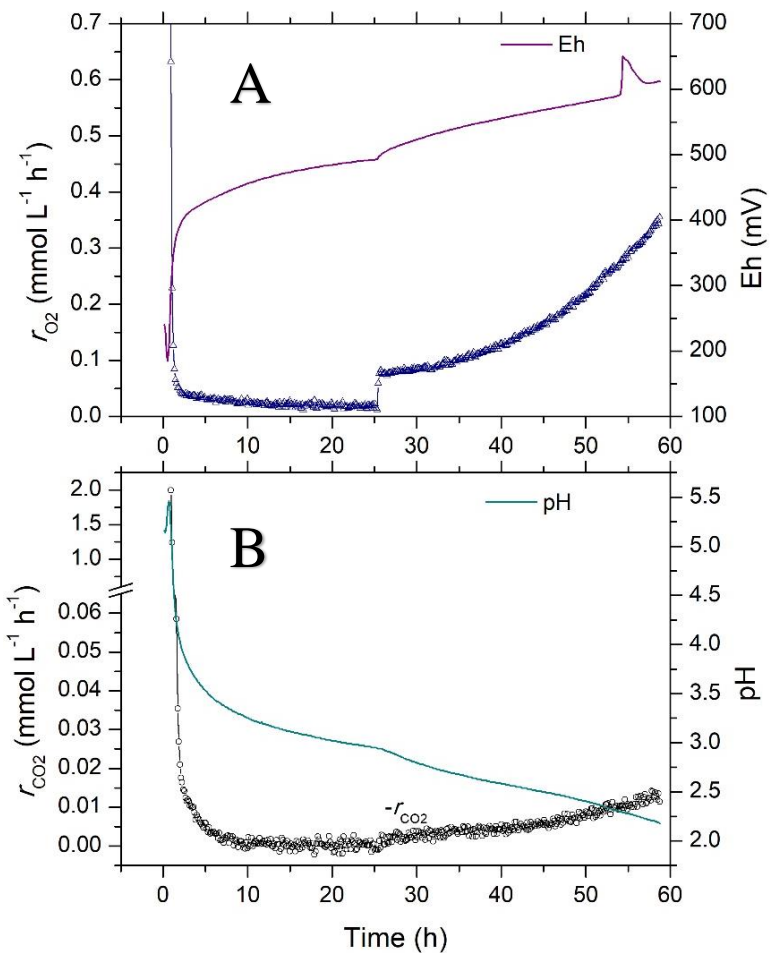


Fig. 9. A Abiotic oxidation of Fe^{2+} in mine water (time period 0-25 h) and the decrease in the rate of iron oxidation due to decreasing pH. Increase in the rate of oxygen consumption (oxidation of Fe^{2+}) after inoculation of iron-oxidizing bacteria ($t = 25$ h) and the subsequent exponential increase in the rate of Fe^{2+} oxidation proportional to the exponential increase in the number of cells per unit volume

B The rate of CO_2 emission (HCO_3^- and dissolved CO_2) from the mine water as a result of lowering the pH and the drop to zero values when the equilibrium state is established with the partial pressure of CO_2 in the atmosphere (in time 10-25 h). After inoculation with Fe -oxidizing bacteria ($t = 25$ h), fixation of CO_2 ($-r_{\text{CO}_2}$) occurs by autotrophic bacteria

Fig. 10 depicts the bacterial oxidation of Fe^{2+} in mine water in batch cultivation (time period 0-30 h) and subsequent continuous cultivation (time period 45-72 h).

After inoculation of the bacterial culture into the actual sample of mine water, the exponential growth of the bacterial cells (specific growth rate $\mu = 0.12 \text{ h}^{-1}$) and the exponential increase in the rate of Fe^{2+} oxidation, culminating in the rate of oxygen consumption $r_{\text{O}_2} = 1.4 \text{ mmol L}^{-1} \text{ h}^{-1}$, which corresponds to the Fe^{2+} oxidation rate of $321 \text{ mg L}^{-1} \text{ h}^{-1}$. Complete oxidation of Fe^{2+} is followed by a sharp decrease in the rate of oxidation to zero ($t = 30$ h) due to substrate exhaustion.

Following this, the bioreactor was switched to continuous flow mode (time period $t = 45$ h) at a dilution rate, $D = 0.12 \text{ h}^{-1}$ that correspond to a hydraulic retention time (HRT) of 8.3 h, using the AMD sample as influent liquor. Two Masterflex® peristaltic pumps were used to pump liquids into and out of the bioreactors to maintain constant liquid volume. With the supply of a new substrate (Fe^{2+}), there was an increase in the rate of oxygen consumption (oxidation of Fe^{2+}). The dilution rate exceeds the critical value, which results in the wash-out effect of bacterial cells from the reactor and a decrease in the rate of Fe oxidation.

In batch cultivation and in continuous systems without fixation of bacterial cells, bacterial Fe^{2+} oxidation values of the order of 500-1000 $\text{mg L}^{-1} \text{h}^{-1}$ were achieved. Compared to a conventional chemostat cultivation with planktonic cells, the bacterial cell washout was apparently accelerated in this system due to cell capturing on the surface of fresh Fe-precipitates with subsequent washing out of these agglomerates from the reactor. The washout of cells from bioreactor modules in continuous flow systems is a potential problem and is usually minimized by including support matrices to act as surfaces for bacterial attachment and immobilization. Grishin and Tuovinen tested glass, resin beads and activated carbon as support matrix materials in fixed-film bioreactors to oxidize Fe^{2+} to Fe^{3+} . Activated carbon displayed the most suitable characteristics for use as a support matrix of *T. ferrooxidans* fixed-film formation. The fastest kinetic performance achieved with the activated-carbon packed-bed bioreactor was 78 g of Fe^{2+} oxidized per liter per h (1,400 mmol of Fe^{2+} oxidized per liter per h) at a true dilution rate of 40 h^{-1} , which represents a hydraulic retention time of 1.5 min (Grishin and Tuovinen, 1988).

Laboratory tests of such devices are currently underway.

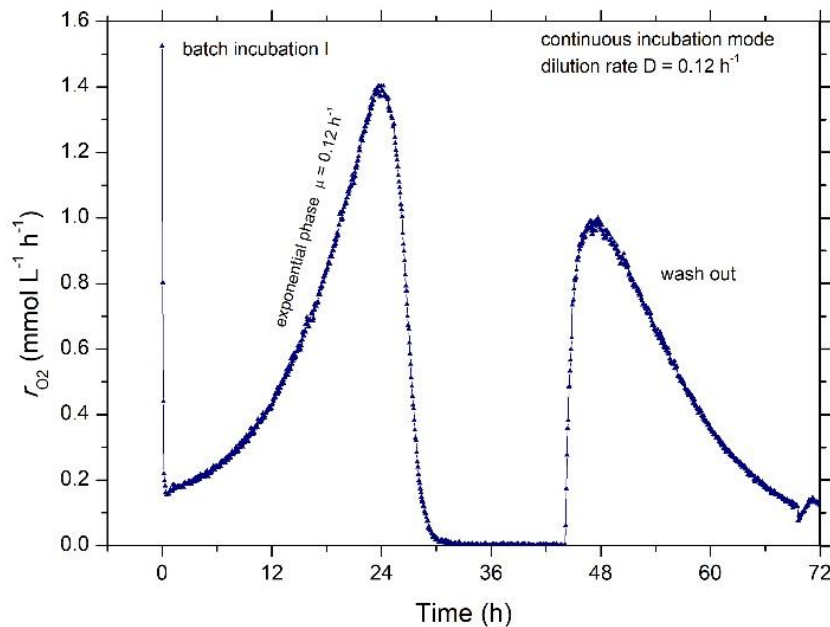


Fig. 10. Bacterial oxidation of Fe^{2+} in mine water in batch culture (time period 0-30 h).

Exponential growth of the bacterial culture $\mu = 0.12 \text{ h}^{-1}$ and exponential increase in the Fe^{2+} oxidation rate culminating in the oxygen consumption rate $r_{\text{O}_2} = 1.4 \text{ mmol L}^{-1} \text{ h}^{-1}$, which corresponds to a Fe oxidation rate of $321 \text{ mg L}^{-1} \text{ h}^{-1}$. Complete oxidation of Fe^{2+} is followed by a sharp decrease in the rate of oxidation to zero ($t = 30 \text{ h}$).

In the time period from $t = 45 \text{ h}$, continuous cultivation took place with the addition of mine water with a dilution rate of $D = 0.12 \text{ h}^{-1}$ (hydraulic retention time 8.33 h). With the supply of a new substrate (Fe^{2+}) there was an increase in the rate of oxygen consumption (oxidation of Fe^{2+})

3.6 Precipitation of Fe-minerals

During the oxidation of Fe^{2+} to Fe^{3+} , the total concentration of dissolved iron in the mine water significantly decreased (Fig. 10.) due to the precipitation of iron hydroxide and the formation of sulfate complexes of trivalent iron (in accordance with equations 1-5).

The amount and composition of the resulting precipitation product depends on the rate of precipitation of individual minerals. Ferric hydroxide precipitates the fastest, which rapidly drains the emerging trivalent iron from the solution and thus prevents the formation of slower-precipitating jarosites. During oxidation with atmospheric air, hydrogen peroxide, and during bacterial oxidation, as well as during neutralization of mine water with NaOH (when determining acidity), we observed

differences in the volume and mass proportion of Fe-precipitates after complete oxidation of Fe^{2+} to Fe^{3+} .

The concentration of monovalent cations directly affects ferric iron solubility within acid sulfate systems (Gramp et al., 2008). Schwertmannite was the predominant phase in the absence of monovalent cations. Jarosites (yellowish precipitates) are formed in the presence of monovalent cations in otherwise similar media. The monovalent cations exercise a major influence on the amount and composition of the precipitate. By comparison to schwertmannite, jarosites contain twice as much S but only about one third of the Fe on a molar basis.

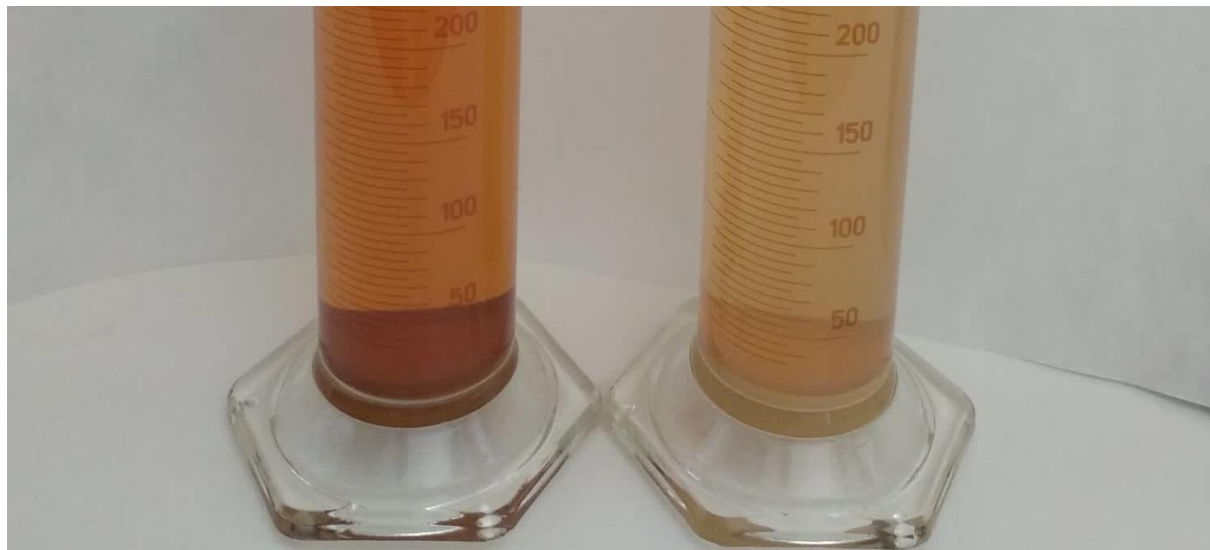


Fig. 11. Sediment volume after bacterial oxidation of Fe^{2+} , precipitation and sedimentation of $\text{Fe}(\text{OH})_3$ on the left and jarosite on the right. Concentration of dissolved Fe^{3+} in the liquid phase: 2357 mg L^{-1} , sample on the left and 1516 mg L^{-1} , sample on the right

3.6.1 Jarosite precipitation



Fig. 11. Sediment after bacterial oxidation of Fe^{2+} in mine water from Nižná Slaná and precipitation of K-jarosite. Fe^{2+} concentration at the beginning 5087 mg L^{-1} . After complete oxidation of Fe^{2+} to Fe^{3+} , the concentration of dissolved Fe^{3+} in the liquid phase was 208 mg L^{-1} , pH 1.9

3.6.2 Mn precipitation

After oxidation and partial precipitation of ferric iron, sodium hydroxide was added in order to increase the pH to 4.05 and facilitate the precipitation of residual ferric iron. The concentration of Fe and Mn in the filtrate after Fe(III) precipitate separation was 6 mg L^{-1} and 510 mg L^{-1} respectively. In the next step potassium permanganate was used to eliminate manganese by oxidative precipitation.

In acid mine water, manganese is present predominantly in the soluble divalent form, and alkalization is a commonly used method for its removal. Non-catalysed oxidation and precipitation of Mn is favoured at high value of pH at about 10 (Sikora et al., 2000). Moreover, during this process manganese co-precipitates with magnesium present in the mine water (Macingova et al., 2016). In this context, oxidative precipitation seems to be a more suitable alternative for manganese removal using different oxidizing agents. To effectively precipitate dilute manganese from solution at lower pH ranges, a powerful oxidizing agent has to be used (Teixeira et al., 2017). Considering our previous experiences (Macingova et al., 2016), an equimolar amount of potassium permanganate was used as a reagent in our experiments. During the process, precipitation of manganese occurred via synproportionation reaction (equation 7). Its concentration in the mine water dropped to a value of 4 mg/l. Simultaneously, a decline of pH from 4.05 to 2.27 and rise of the ORP value from 552 mV to 934 mV were recorded.



The morphology and elemental composition of obtained products were studied by scanning electron microscopy (SEM) and energy dispersive X-ray spectroscopy (EDX). The recovery efficiencies of Fe and Mn from mine water reached 99.87 % and 99.25%, respectively.

The next step is the reversible adsorption of Ni using chelating sorbents with the possibility of regeneration. In the last step, reverse osmosis is used to obtain a concentrated solution of MgSO_4 and pure water (permeate).

3.6.3 Recovery of Ni and other elements

For the absorption of metal ions, four types of adsorbents were used: 1. silica spheres with amino groups, 2. silica mesoporous materials with mercapto groups, 3. silica adsorbents with EDTA groups, and 4. commercial chelating resin DOWEXTM M4195 for copper, nickel, and cobalt processing with bis-picolyamine multi-dentate amine ligand. Sorption was carried out in dynamic mode for 24 hours at room temperature with an adsorbent concentration of 1 g/L. Preliminary laboratory tests with mine water samples showed lower adsorption efficiency at low pH (2.2) compared to recovery achieved at neutral and weakly alkaline pH. The laboratory tests are currently underway.

4 Conclusions

In this work we proposed two active approaches to treat MIWs flowing out from the former mining plant Siderit Nižná Slaná. The effluent water is significant for its high mineralisation values and especially high Fe content, that causes a significant red coloration of the Slaná river.

In the first approach, oxidation of Fe^{2+} to Fe^{3+} is mediated by Fe-oxidizing bacteria followed by precipitation of ferric minerals. The second process is without oxidation step, using lime to neutralize the acidity and precipitate Fe^{2+} in the form of $\text{Fe}(\text{OH})_2$.

In this process, the main focus is on the high value constituents recovery (Mn, Ni, Co,) and water purification from other toxic elements (As, Cd).

The effluent would then enter constructed wetland where the residual metals and sulfate precipitation occur by various alkalinity generating processes mediated by diverse biological systems.

Due to AMD's highly saturated nature with respect to ferric iron (oxy)hydroxides and alkali metal jarosites, the passive treatment with anoxic limestone drains had to be omitted.

While MIW is harmful to the environment, it could also contain significant amounts of valuable metals which recovery could be profitable. Some of these metals, such as Ni, Co, Mn have a great economic importance according to the report on critical raw materials supply for EU countries published by the European Commission in March 2023 (Directorate-General for Internal Market, 2023). The recovery of these metals from MIW not only reduces environmental impacts but also provides a source of valuable resources (European et al., 2019).

Numerous field/laboratory techniques, model and code development grew out of considerable research on groundwater geochemistry, mine waste geochemistry, reactive-transport studies and

cooperative interaction between researchers, regulatory agencies and industry. The challenge of complex mine site remediation is best met with continued cooperation between research and remediation (Nordstrom et al., 2015).

Declaration of Competing Interest

The authors declare that they have no known competing financial interests or personal relationships that could have appeared to influence the work reported in this paper

Acknowledgements

This study was supported by the Slovak Grant Agency (VEGA), Grant No. 2/0108/23. Slovak Research and Development Agency under the contract No. APVV-20-0140

References

Brahaita, I.-D. et al., 2017. THE EFFICIENCY OF LIMESTONE IN NEUTRALIZING ACID MINE DRAINAGE – A LABORATORY STUDY. Carpathian journal of earth and environmental sciences, 12: 347-356.

Direktorat-General for Internal Market, I., Entrepreneurship and SMEs, 2023. Study on the Critical Raw Materials for the EU 2023 - Final Report.

European, C. et al., 2019. Recovery of critical and other raw materials from mining waste and landfills : state of play on existing practices. Publications Office.

García, C., Moreno, D.A., Ballester, A., Blázquez, M.L. and González, F., 2001. Bioremediation of an industrial acid mine water by metal-tolerant sulphate-reducing bacteria. Minerals Engineering, 14(9): 997-1008.

Gramp, J.P., Jones, F.S., Bigham, J.M. and Tuovinen, O.H., 2008. Monovalent cation concentrations determine the types of Fe(III) hydroxysulfate precipitates formed in bioleach solutions. Hydrometallurgy, 94(1-4): 29-33.

Grishin, S.I. and Tuovinen, O.H., 1988. Fast kinetics of fe oxidation in packed-bed reactors. Appl Environ Microbiol, 54(12): 3092-100.

Herrera, L., Ruiz, P., Aguillon, J.C. and Fehrmann, A., 1989. A new spectrophotometric method for the determination of ferrous iron in the presence of ferric iron. Journal of Chemical Technology & Biotechnology, 44(3): 171-181.

Johnson, D.B. and Hallberg, K.B., 2005. Acid mine drainage remediation options: a review. Science of The Total Environment, 338(1): 3-14.

Kirby, C.S. and Cravotta, C.A., 2005. Net alkalinity and net acidity 2: Practical considerations. Applied Geochemistry, 20(10): 1941-1964.

Macingova, E., Ubaldini, S. and Luptakova, A., 2016. Study of Manganese Removal in the Process of Mine Water Remediation. Inzynieria Mineralna, 1: 121-128.

Mogashane, T.M., Maree, J.P., Mujuru, M. and Mphahlele-Makgwane, M.M., 2020. Technologies that can be Used for the Treatment of Wastewater and Brine for the Recovery of Drinking Water and Saleable Products, Recovery of Byproducts from Acid Mine Drainage Treatment, pp. 97-156.

Nordstrom, D.K., Blowes, D.W. and Ptacek, C.J., 2015. Hydrogeochemistry and microbiology of mine drainage: An update. Applied Geochemistry, 57: 3-16.

Sikora, F.J., Behrends, L.L., Brodie, G.A. and Taylor, H.N., 2000. Design Criteria and Required Chemistry for Removing Manganese in Acid Mine Drainage Using Subsurface Flow Wetlands. Water Environment Research, 72(5): 536-544.

Singer, P.C. and Stumm, W., 1970. Acidic mine drainage: the rate-determining step. Science, 167(3921): 1121-3.

Teixeira, L.A.C., Queiroz, J.P.L. and Marquez-Sarmiento, C., 2017. Oxidative Precipitation of Manganese from Dilute Waters. Mine Water and the Environment, 36(3): 452-456.